Electron Cloud Buildup Models and Plans

Jim Crittenden
Cornell Laboratory for Accelerator-Based Sciences and Education
LCWS11
29 September 2011

EC buildup modeling over > 15 years – broadbased collaborative effort --

Example

ECLOUD'10

49th ICFA Advanced Beam Dynamic Workshop on Electron Cloud Physics

8-12 October 2010

M.A.Furman: Electron Cloud Buildup Simulations for the ILCDRs: Antechamber Benefit

T.Demma: Electron Cloud Buildup and Instability in DAΦNE

J.R. Calvey: Methods for Quantitative Interpretation of RFA Data

D.L.Kreinick: Using Coherent Tune Shifts to Evaluate Electron Cloud Effects on Beam Dynamics at CESRTA

L.Wang: Electron Cloud Trapping in Quadrupole and Sextupole Magnets

L.Boon: Analysis of Synchrotron Radiation Using SYNRAD3D and Plans to Create a Photoelectron Model

G.Dugan: SYNRAD3D Photon Propagation and Scattering Simulation

JAC: Electron Cloud Modeling for Shielded Pickup Measurements at CESRTA

C.Celata: Electron Dynamics in the Wigglers of CESRTA

P.LeBrun: Simulation of the Electron Cloud in the FNAL Main Injector Using VORPAL

S.Veitzer: Modeling Electron Cloud Buildup and Microwave Diagnostics with VORPAL

K.Harkay: Electron Cloud Issues for the APS Superconducting Undulator

Modeling Coherent Tune Shift Measurements
PAC09, IPAC10, PAC11, IPAC11

POSINST simulations with direct radiation rates, reflectivity=15%, QE=12%, Gaussian PE energy spectrum

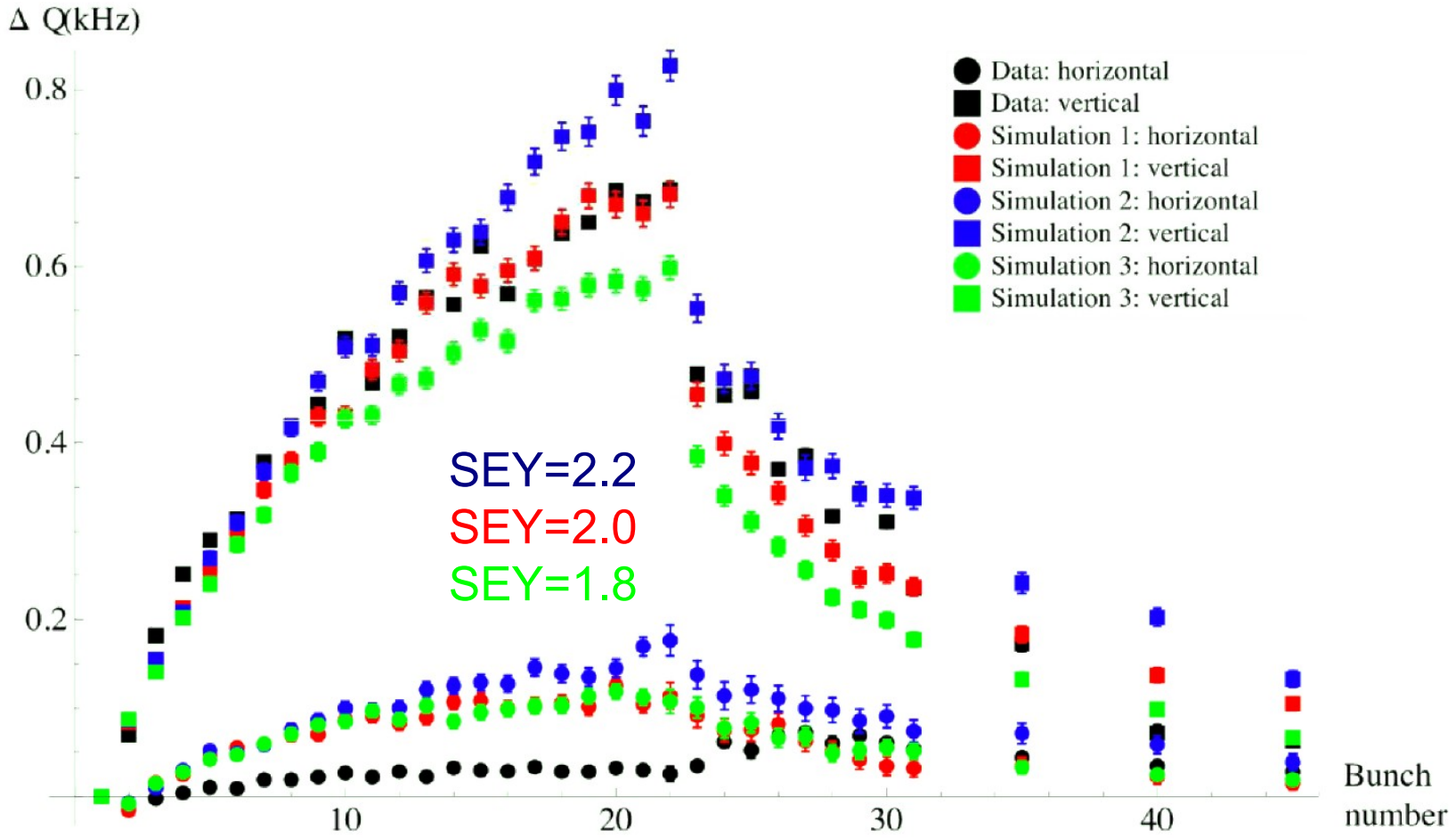

ILC DR Coherent Tune Shift Calculation

JAC & K.Sonnad, PAC11, WEP110

Synchrotron Radiation Pattern in the DSB3 Lattice Arcs

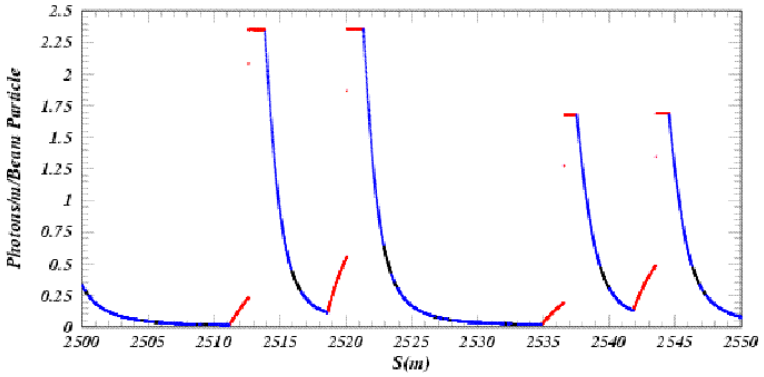

Element-type-specific beta functions and photon rates from BMAD/SYNRAD

Element	Tot Length [m]	Ring Fraction	<Beta X> [m]	<Beta Y> [m]	<Sig X> [mm]	<Sig Y> [mm]	<Photon Rate> [Phot/m/e] Outside	Inside
Dipole	324.2	10.0%	3.6	18.6	0.1207	0.0166	1.083	0.000
Drift	2560.8	79.1%	33.3	31.8	0.2269	0.0210	0.145	0.027
Wiggler	101.9	3.1%	10.8	14.1	0.0899	0.0145	0.729	0.719
Quadrupole	206.8	6.4%	21.5	23.4	0.2897	0.0177	0.236	0.067
Sextupole	44.3	1.4%	20.7	25.3	0.4207	0.0191	0.129	0.000
Non-dipole	2913.8	90.0%	31.5	30.5	0.2295	0.0205	0.171	0.053
Non-drift	677.2	20.9%	11.3	19.8	0.1873	0.0168	0.709	0.129
Total	3238.1	100.0%	28.7	29.3	0.2186	0.0201	0.263	0.048

Table 1: Element-type-specific ring lengths, and averages of beta functions, beam sizes, and photon rates on the outside and inside walls of the vacuum chamber for the DSB3_2 ILC damping ring lattice design

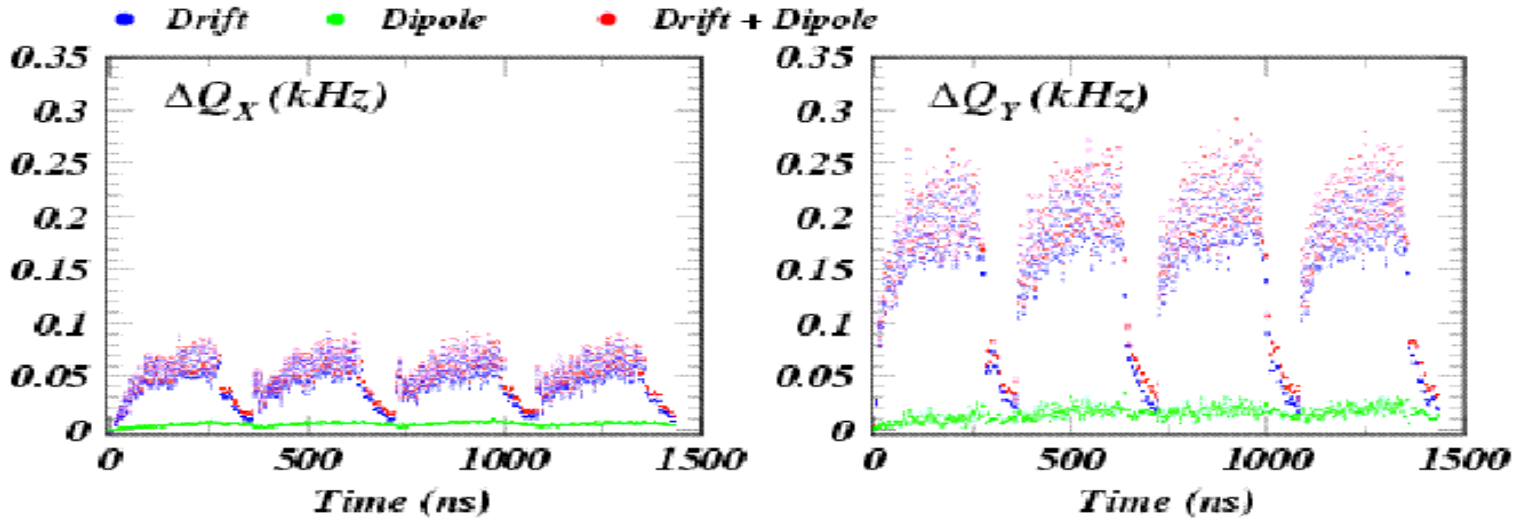

Coherent Tune Shifts Calculated from Field Gradients Along Four 45-Bunch Trains
Contributions from drift and dipole regions
Compare to the fractional design tunes of 17.5 kHz and 22.3 kHz.

EC Buildup R&D at CESRTA

- CESR Configuration
  - Damping ring layout
  - 4 dedicated EC experimental regions
  - Upgraded vacuum/EC instrumentation
  - Energy flexibility from 1.8 to 5.3 GeV
  - Regularly achieving <10pm vertical emittance
- EC Diagnostics and Mitigation
  - ~30 RFAs presently deployed
  - TE wave measurement capability in each experimental region
  - Time-resolved shielded pickups in 3 experimental locations (2 with transverse information)
  - Over 20 individual mitigation studies conducted in Phase I
    - 20 chambers
    - 2 sets of in situ SEY measurements
    - Follow-on studies in preparation for Phase II extension of program
- Simulations: to allow extrapolation to ILC DR
  - Simulations of photon transport, including scattering (specular and diffuse) and fluorescence, in realistic chambers (including antechambers).
  - EC growth: establishing physics model parameters for EC growth codes (POSINST, ECLOUD): models of primary photoemission and secondary emission

EC Buildup Detectors at CESRTA

L3 Electron cloud experimental region

PEP-II EC Hardware:

Chicane, upgraded SEY station (commissioning in May 2009)

Drift and Quadrupole diagnostic chambers

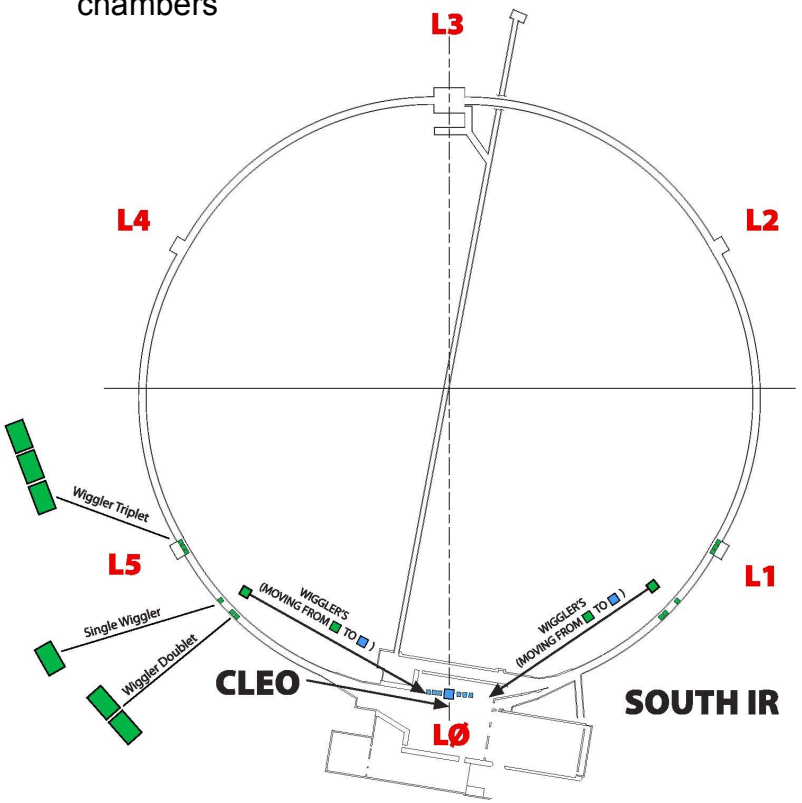

New electron cloud experimental regions in arcs (after 6 wigglers moved to L0 straight)

Locations for collaborator experimental vacuum chambers

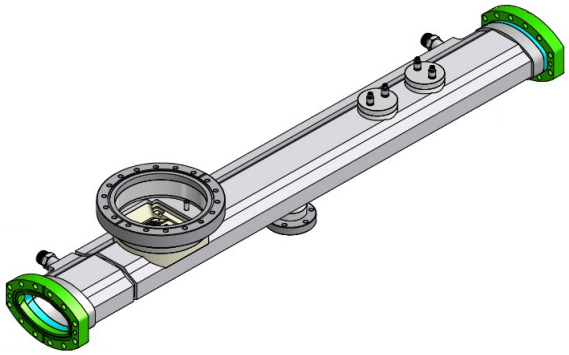

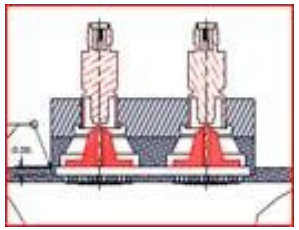

30 RFAs in drift regions, dipoles, quadrupoles, and wigglers

Custom vacuum chambers with shielded pickup detectors

Uncoated aluminum, and TiN, amorphous carbon, diamond-like carbon coatings

Drift Region RFA Data vs Simulation

J.R. Calvey et al, ECLOUD10, PaC11, IPAC11

Goals:

Evaluate surfaces under a wide range of conditions to evaluate in situ surface parameters using the RFA data

- Use photon distributions from 3d photon transport simulations
- Vary: Bunch charge & spacing, species, beam energy, RFA retarding voltage
- Fit for:
  - Peak value of the true SEY
  - Energy of the SEY peak
  - Elastic scattering fraction, $\delta(0)$
  - Rediffused scattering fraction
  - Quantum efficiency
- Incorporate constraints from time-resolved shielded pickup (SPU) data

5.3 GeV Data

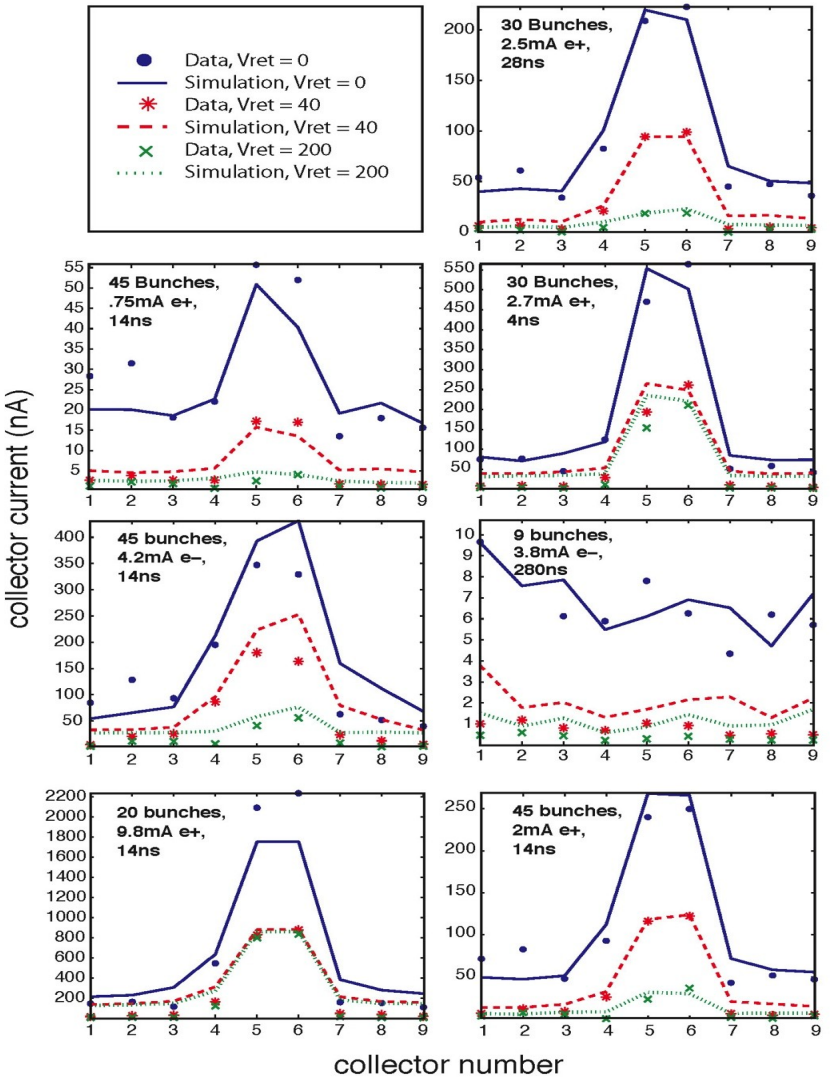

ECLOUD Modeling of CESRTA Shielded Pickup Pulse Shapes: Photoelectrons

JAC et al, IPAC11, WEPC135, *Recent Developments ...*

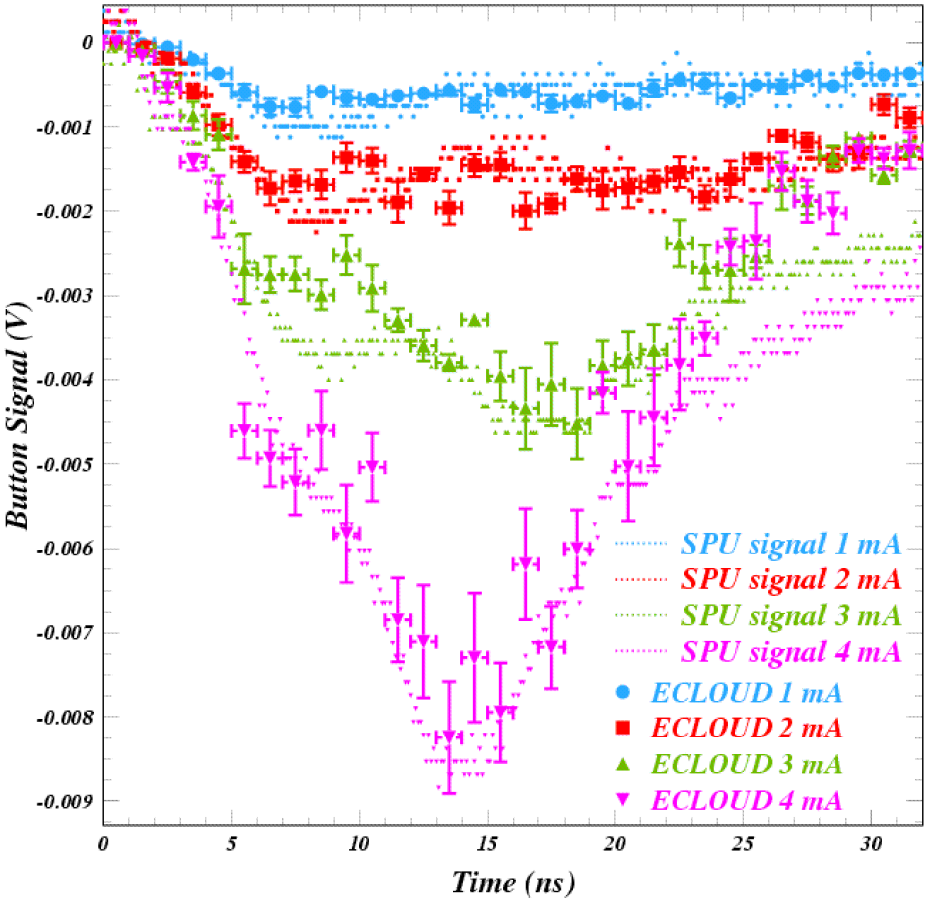

Disentangling the Photoelectron Production Kinetic Energy Distribution from the Beam Kick Strengths

The early SPU signal from the leading bunch for a positron beam is largely due to photoelectrons produced on the bottom of the vacuum chamber. This is the closest production point where the beam kick attracts the photoelectrons toward the SPU. Thus the size and shape of the leading bunch signal is determined by the reflected photon rate, azimuthal distribution, the quantum efficiency for producing photoelectrons, and the kinetic energy distribution of the photoelectrons. In particular, the arrival time distribution determines the shape. By modeling the shape for different strengths of beam kick, we can determine the photoelectron energy distribution. An example of such an analysis is shown on the left. Note that the signal begins just a few nanoseconds after bunch passage even for weak beam kicks, indicating that high-energy photoelectrons were produced (hundreds of eV).

Example: 3 mA/bunch 5.3 GeV e+ 15E a-Carbon

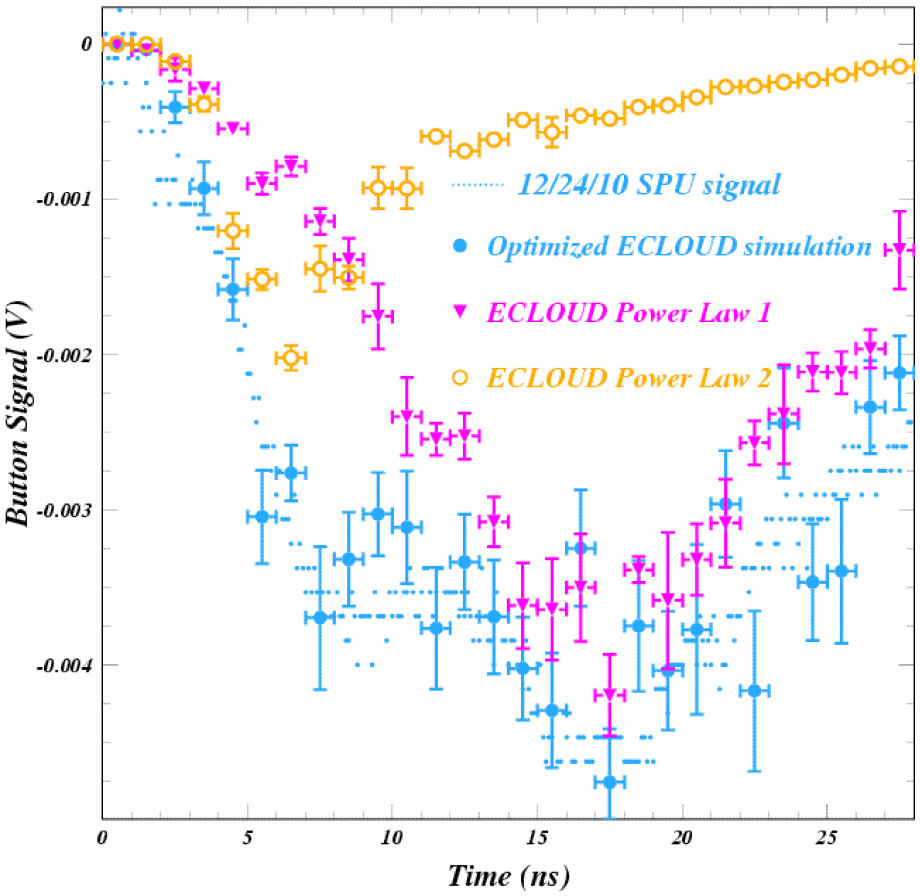

Two Power-Law Contributions

$$F(E) = E^{P1} / (1 + E/E_0)^{P2}$$

$$E_0 = E_{peak} \ (P_2-P_1)/P_1$$

This level of modeling accuracy was achieved with the photoelectron energy distribution shown below, using a sum of two power law distributions.

$$E_{peak} = 80\ eV \quad P_1 = 4 \quad P_2 = 8.4$$

The high-energy component (22%) has a peak energy of 80 eV and an asymptotic power of 4.4. Its contribution to the signal is shown as yellow circles in the lower left plot.

$$E_{peak} = 4\ eV \quad P_1 = 4 \quad P_2 = 6$$

The low-energy component (78%) has a peak energy of 4 eV and an asymptotic power of 2. It's contribution to the signal is shown as pink triangles.

Photoelectron Energy Distribution
5.3 GeV e+ 15E a-Carbon

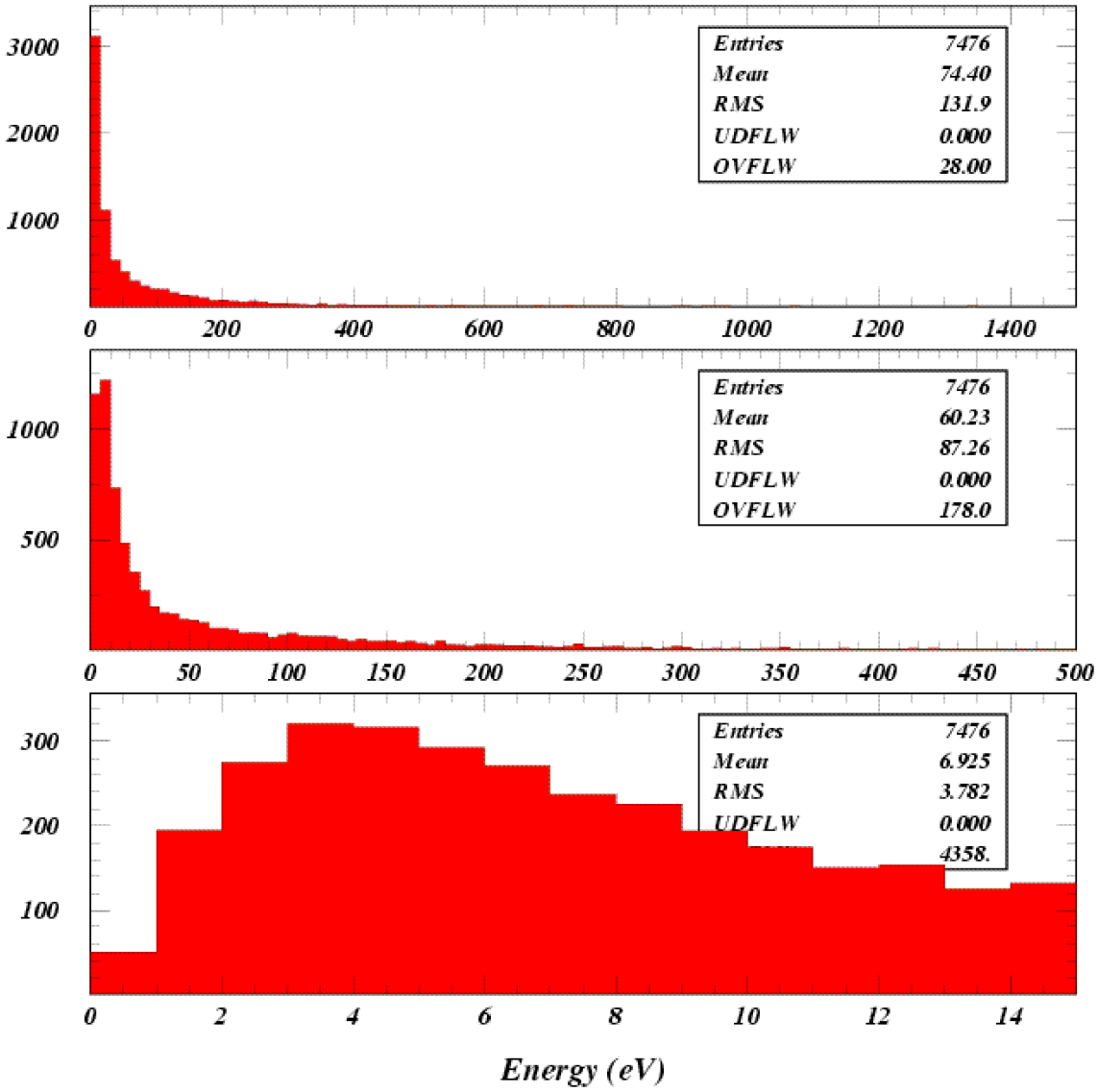

ECLOUD Modeling of CESRTA Shielded Pickup Pulse Shapes: Secondary electrons

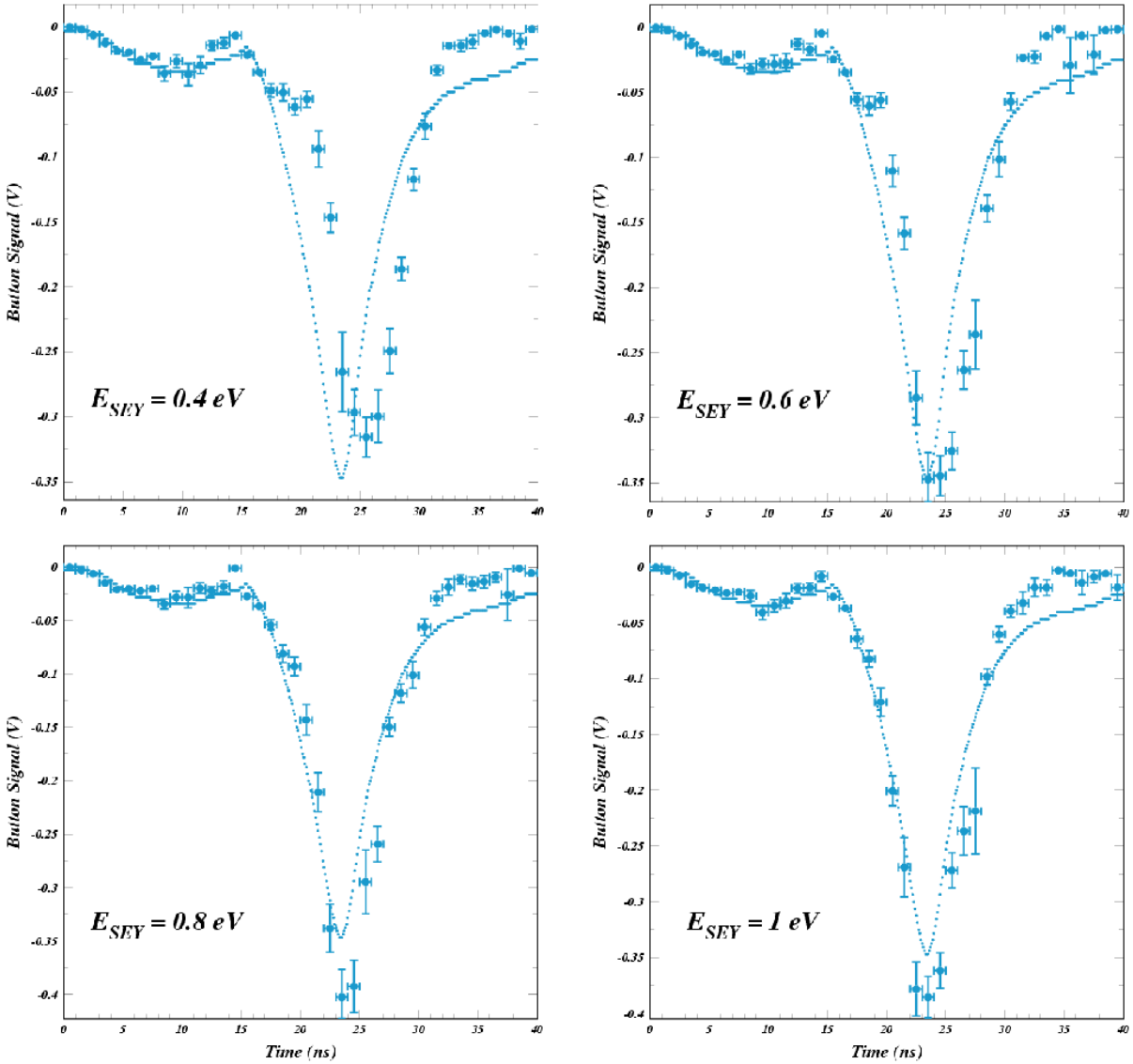

Constraints on the kinetic energy distribution for secondary electrons

$$f(E_{sec}) \sim E_{sec} \exp(-E_{sec}/E_{SEY})$$

A Lower Bound on the E_{SEY} Parameter

The signal from a witness bunch following 14 ns after the leading bunch includes additionally a much larger contribution from secondary cloud electrons accelerated into the SPU detector by the witness-bunch kick.

The figures on the left show that if the secondary energy distribution does not include sufficiently high energies, the modeled 14-ns witness bunch signal shape is distorted and inconsistent with the measured signal.

In Situ Vacuum Chamber Comparisons – Conditioning Effects --

JAC et al, IPAC11, WEPC135, *Recent Developments ...*

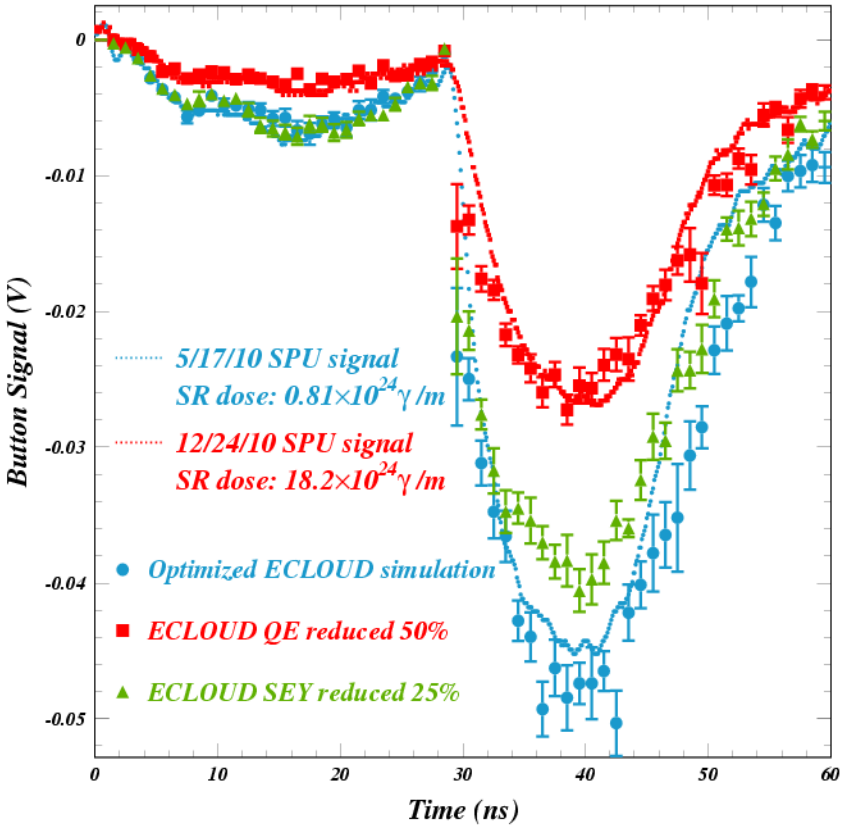

Beam Conditioning in an Amorphous-carbon-coated Al Chamber

Shielded pickup signals measured in an amorphous-carbon-coated chamber in May (blue dotted line) and December (red dotted line) of 2010 for two bunches carrying 4.8×10^{10} 5.3 GeV positrons 28 ns apart. The synchrotron radiation dose increased by a factor of twenty during this time interval. The ECLOUD model optimized for the May data is shown as blue circles, the error bars showing the model statistical uncertainties.

The leading bunch arises from photoelectrons produced on the bottom of the vacuum chamber. Careful tuning of the energy distribution and quantum efficiency for photoelectrons produced by reflected photons is required to reproduce its size and shape. The signal from the witness bunch includes additionally the contribution from secondary cloud electrons accelerated into the SPU detector by the witness bunch kick and is therefore crucially dependent on the secondary yield and production kinematics. Since the conditioning affects both signals similarly, we can conclude that the conditioning change is in the quantum efficiency rather than in the secondary yield.

The December measurement is reproduced by a 50% decrease in the modeled quantum efficiency for photoelectron production. A reduction in the secondary yield of 25% is inconsistent with the observed effect, since the leading bunch signal is unchanged.

In Situ Vacuum Chamber Comparisons – Coating Comparison --

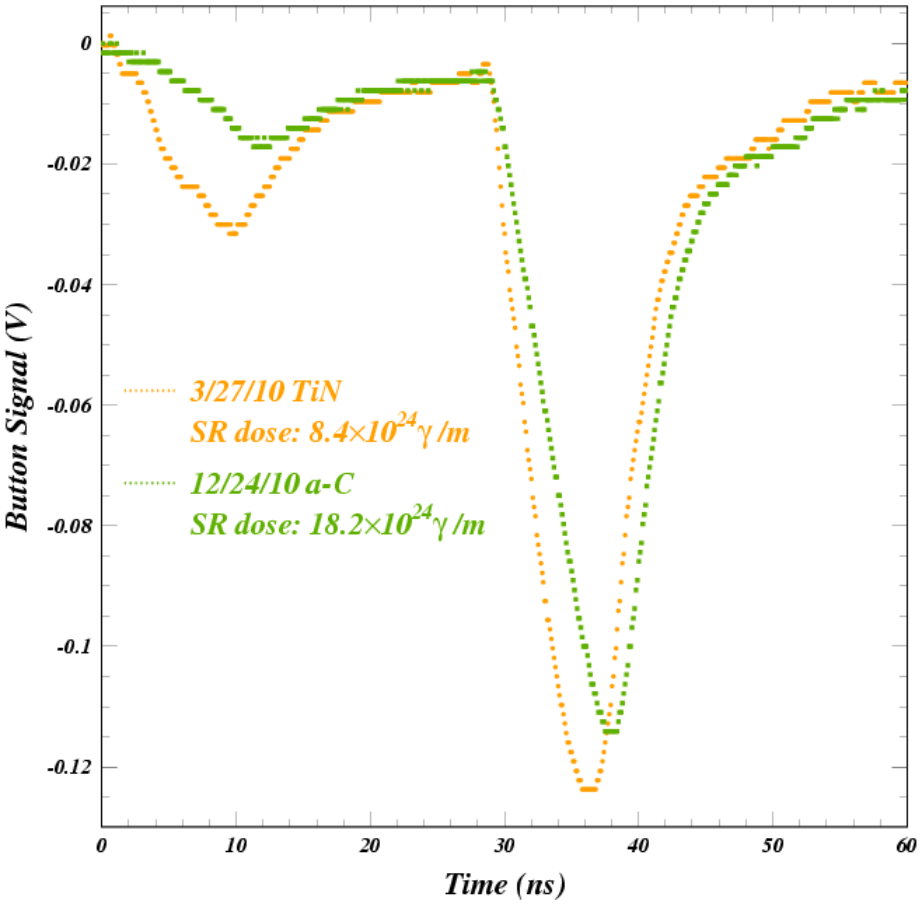

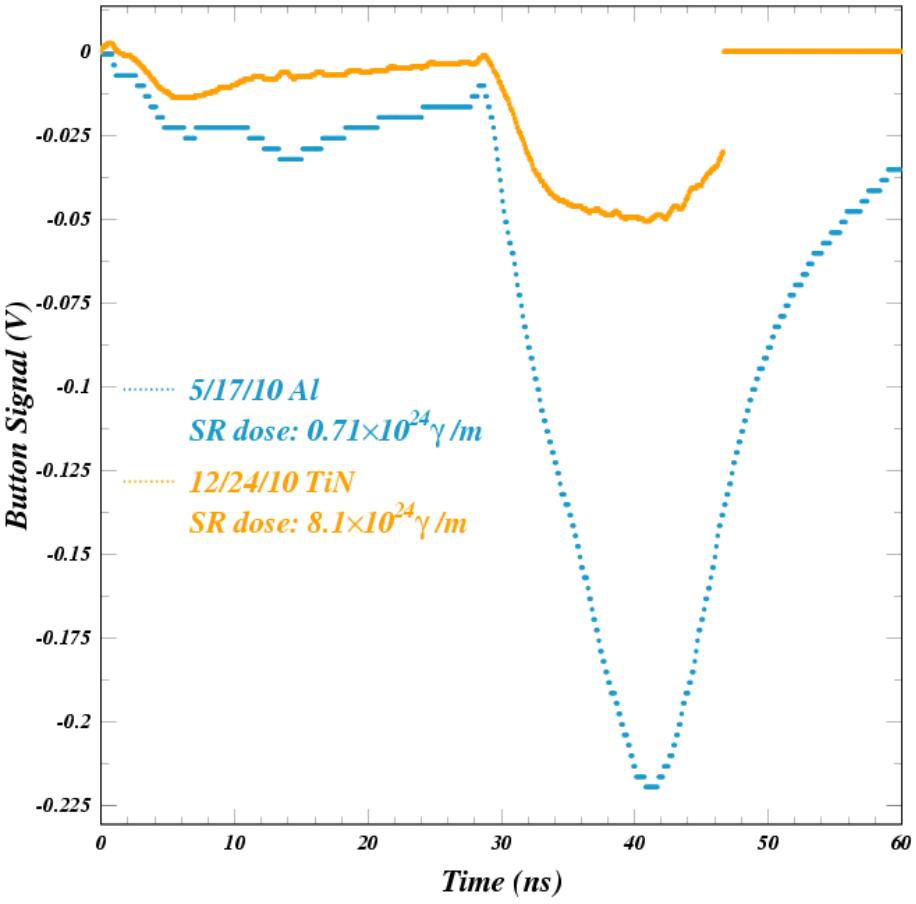

The carbon coating suppresses photoelectron production relative to the TiN coating, especially at high photoelectron energy. However, the secondary yield is somewhat higher.

The quantum efficiency for reflected photons and the secondary yield are both much smaller for conditioned TiN than for uncoated aluminum.

Shielded Pickup Witness Bunch Studies for Determining Cloud Lifetime

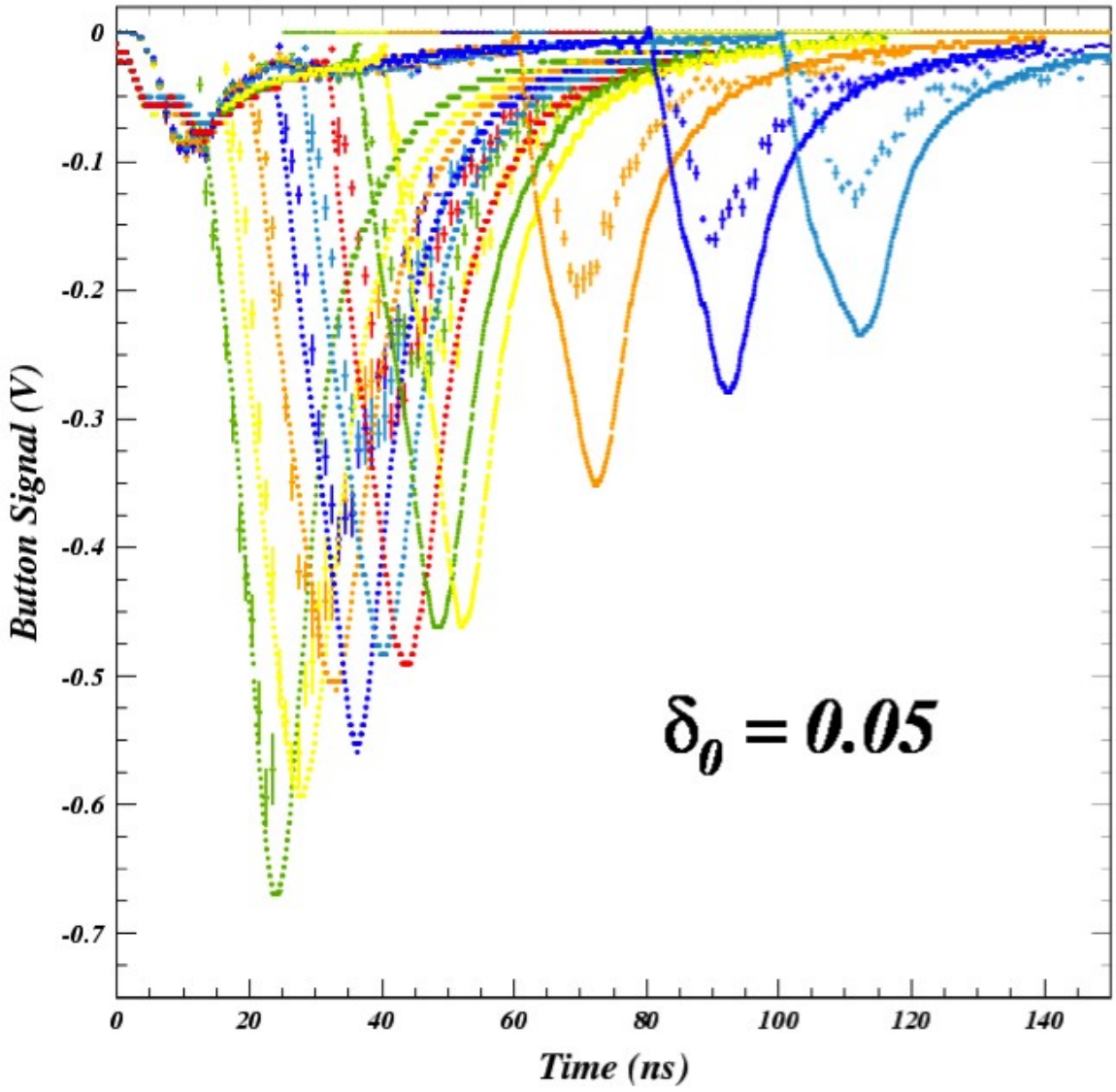

Superposition of eleven two-bunch SPU signals with time delays between 12 and 100 ns, compared to the ECLOUD model result

The cloud lifetime following passage of the final bunch is determined by the elastic secondary process, because it dominates at low incident electron energy, while the true and rediffused secondary processes both produce secondaries with reduced energy.

This was the original motivation for the shielded pickup development and was the analyis of first priority. These analyses have shown cloud lifetimes for the coated chambers (TiN, amorphous carbon, and diamond-like carbon) to be dramatically shorter than for the uncoated aluminum chamber.

This early study shows discrepancies with the measured signals which were later found to be due to an unrealistic model for photoelectron production. Despite these deficiencies in the model, the conclusion that an elastic yield value of 0.05 is too low for this uncoated aluminum chamber is clear.

Determining the Elastic Yield Parameter δ_0 – Compare uncoated Al with TiN coating--

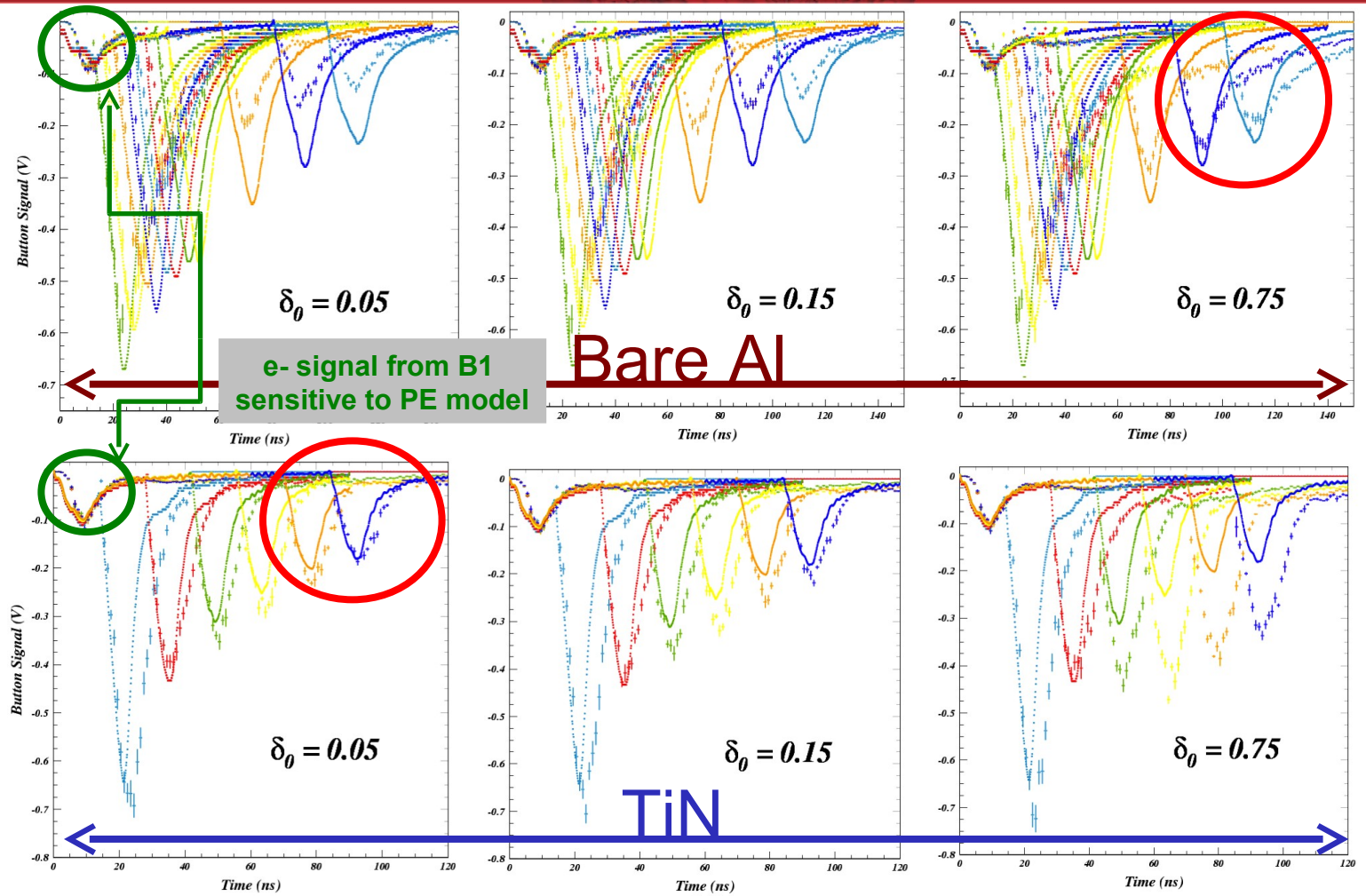

Witness bunch studies with delays up to 100 ns show clear sensitivity to the secondary elastic yield parameter, giving a value of about 0.75 for bare aluminum and about 0.05 for the TiN coating. The discriminating power is independent of the photoelectron model.

Planned Improvements to EC Growth Simulations

- **Better photon reflection and transport model needed for simulations and data analysis**
- **Synrad3D (Sagan, et al.) answers this need, but work remains**
  - **Fully validate CESRTA vacuum chamber geometries, then implement ILC DR designs**
  - **Incorporate diffuse scattering due to surface roughness and fluorescence**

Photon distribution vs angle

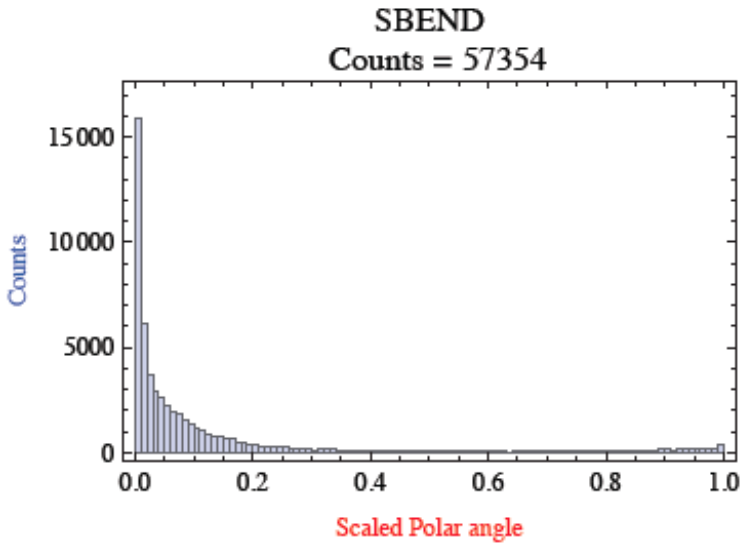

Electron cloud distribution vs position,after 10 bunch train

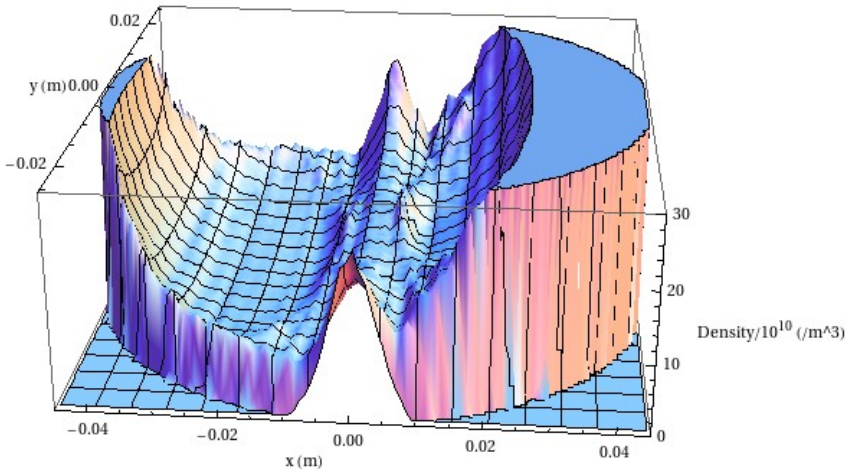

Time-resolved SPU measurements indicate that we also need to have a better photoelectron model (fitting of RFA data also requires this)